The hemopexin domain of MMP3 is responsible for mammary epithelial invasion and morphogenesis through extracellular interaction with HSP90β

Ana Luísa Correia,[1,2] Hidetoshi Mori,[1] Emily I. Chen,[3] Fernando C. Schmitt,[4] and Mina J. Bissell[1,5]

[1]Life Sciences Division, Lawrence Berkeley National Laboratory, Berkeley, California 94720, USA; [2]Graduate Program in Areas of Basic and Applied Biology, Abel Salazar Biomedical Sciences Institute, University of Porto, 4050-313 Porto, Portugal; [3]Department of Pharmacological Sciences and Proteomics Center, Stony Brook University, Stony Brook, New York 11794, USA; [4]Medical Faculty of Porto, Institute of Molecular Pathology and Immunology, University of Porto, 4200-465 Porto, Portugal

Matrix metalloproteinases (MMPs) are crucial mediators in sculpting tissue architecture and are required for many physiological and pathological processes. MMP3 has been shown to regulate branching morphogenesis in the mammary gland. Ectopic expression of proteolytically active MMP3 in mouse mammary epithelia triggers supernumerary lateral branching and, eventually, tumors. Using a three-dimensional collagen-I (Col-1) gel assay that simulates epithelial invasion and branching, we show that it is the hemopexin domain that directs these processes. Using three different engineered constructs containing a variation on MMP3 structural domains, we confirmed the importance of the hemopexin domain also in primary organoids of the mammary gland. A proteomic screen of MMP3-binding partners surprisingly revealed that the intracellular chaperone heat-shock protein 90 β (HSP90β) is present extracellularly, and its interaction with the hemopexin domain of MMP3 is critical for invasion. Blocking of HSP90β with inhibitory antibodies added to the medium abolished invasion and branching. These findings shift the focus from the proteolytic activity of MMP3 as the central player to its hemopexin domain and add a new dimension to HSP90β's functions by revealing a hitherto undescribed mechanism of MMP3 regulation. Our data also may shed light on the failure of strategies to use MMP inhibitors in cancer treatment and other related disorders.

Prior to the defining functions of the mammary gland (i.e., pregnancy and lactation), the female mammal develops an epithelial tree through branching morphogenesis. During this process, epithelial cells have to mobilize the necessary machinery for invasion of the growing ducts into the fat pad and the formation of secondary and tertiary branches to complete the eventual adult mammary architecture. It has been shown that the success of this process relies on the activities of a number of matrix metalloproteinases (MMPs) (Fata et al. 2004; Khokha and Werb 2011). Paradoxically, the loss of mammary structure also is dependent on MMPs. Indeed, we showed two decades ago that during the process of involution, up-regulation of MMP3 is responsible for the collapse and remodeling of the alveoli of lactating mice, indicating the intimate connection between functional differentiation and tissue structure (Talhouk et al. 1991, 1992). Conditional activation of MMP3 in functionally normal mouse mammary epithelial cells led to cleavage of E-cadherin and epithelial-to-mesenchymal transitions (EMT) (Lochter et al. 1997a). We also showed that ectopic expression of constitutively active MMP3 in mammary epithelia enhanced lateral branching and induced precocious alveolar development in virgin mice (Sympson et al. 1994). As these animals aged, the stroma was profoundly altered in both structure and function (Thomasset et al. 1998), and mice eventually developed mammary tumors that exhibited chromosomal aberrations (Sternlicht et al. 1999). The mechanism involved a change in the cytoskeleton and cell shape through induction of RAC1B, a spliced isoform of RAC1 found in human breast tumors (Schnelzer et al. 2000). Addition of MMP3 or the expression of RAC1B also led to formation of reactive oxygen species (ROS) and genomic instability (Radisky et al. 2005).

[5]Corresponding author
Email mjbissell@lbl.gov

Because the proteolytic activity of MMPs resides within the catalytic domain, it has been generally assumed that this domain is responsible for all of the functions of MMPs. More recently, some biochemical literature has indicated that the noncatalytic domains of certain MMPs, such as MMP9, MMP12, and MMP14, may also have activities in mammalian cell lines (Mori et al. 2002; Wang et al. 2004; Dufour et al. 2008; Sakamoto and Seiki 2009). The failure of clinical trials based on inhibitors of MMP catalytic domains (Overall and Kleifeld 2006) suggested to us that the other domains of MMP3 may have functions in invasion and possibly cancer.

Here we show that overexpression of MMP3 constructs without catalytic activity is sufficient to direct mammary epithelial invasion in collagen-I (Col-1) gels. Additionally, the functional activity requires the surprising interaction of heat-shock protein 90 β (HSP90β) with MMP3 in the extracellular milieu. This interaction is necessary for invasion and branching in not only cultured cells, but also primary organoids where the mammary architecture remains intact. We believe that these findings introduce an alternative to the classic paradigm of MMP3 activity and point to an HSP90β-mediated regulation of MMP3 function essential for epithelial invasion and mammary morphogenesis.

Results

The hemopexin domain of MMP3 is required for a change in cell shape in two-dimensional (2D) substrata and invasion in Boyden chambers

To investigate the function of different domains of MMP3, we engineered three Flag-tagged constructs containing different domains of the MMP3 molecule: the full-length (FL) MMP3, a mutant lacking the hemopexin-like domain (dPEX), and a construct containing a point mutation, E219A (EA), at the catalytic core (Fig. 1A). We overexpressed the distinct MMP3 constructs in SCp2 (Fig. 1B), a mammary cell line shown to undergo EMT upon expression of MMP3 (Lochter et al. 1997a; Radisky et al. 2005). SCp2 cells have a low level of endogenous MMP3 activity that resembles that found in vivo in mammary epithelia; we chose to maintain this activity advisedly to have a positive control for the overexpression of the human homologs in murine cells. This was additionally useful because we observed that the concurrent knockdown of endogenous MMP3 and the introduction of the exogenous levels of the human constructs would lead to aberrant cell behavior. To compare the cultures transduced with different constructs with each other and with the control, we ensured that the endogenous as well as the exogenous levels of MMP3 were comparable in all engineered cell lines (Supplemental Fig. S1). Overexpression of the exogenous constructs in SCp2 showed that the proteolytic activity (measured by casein-quenched degradation) in dPEX was similar to FL and that they both were higher than EA-SCp2 or control cells (Fig. 1C).

Cell scattering is a functional consequence of EMT (Vincent-Salomon and Thiery 2003); overexpression of

FL-MMP3 induced scattering in 2D cultures (Fig. 1D, first and second rows). The EA mutant also stimulated a spindle-shaped morphology and scattered phenotype, albeit to a lower extent (Fig. 1D, third row). In contrast, dPEX-SCp2 did not scatter and resembled the control cultures (Fig. 1D, fourth row). We and others showed that E-cadherin is a substrate for MMP3, and its loss is associated with scattering (Lochter et al. 1997a; Noe et al. 2001). Consistent with these observations, we found that FL and dPEX-MMP3 both reduced the expression of E-cadherin (Fig. 1E, second and fourth rows) by shedding its extracellular domain (Supplemental Fig. S2A). Surprisingly, however, EA-SCp2 cells (which lack the proteolytic activity) still exhibited a stretched phenotype even in the presence of E-cadherin levels similar to control cultures (Fig. 1E, third row), suggesting that the ability of MMP3 to disrupt epithelial morphology was due to activities residing in its other domains.

Using changes in cell morphology and reorganization of filamentous actin (F-actin) as additional endpoints, we observed that in dPEX-SCp2 and control cultures, F-actin was predominantly organized in cortical bundles, and cells had a classical epithelial morphology in 2D (Fig. 1F, first and last rows). In sharp contrast, actin filaments were extended in FL and EA-SCp2 cultures, and cells were elongated (Fig. 1F, second and third rows). We quantified these morphological changes by calculating the ratio of the longest (length) to the shortest (width) axis of the cell, which we refer to as the cellular elliptical factor (Fig. 1G). Whereas FL and EA-SCp2 displayed an elliptical factor >2, cells expressing control vector or dPEX had elliptical factors close to 1. These observations show a critical role for the MMP3 hemopexin domain in altering epithelial cell shape.

Despite the small amount of proteolytic activity of SCp2 cells, these exhibit little invasive behavior (Lochter et al. 1997b); the same is true in SCp2 cells transduced with control vector (Fig. 1H, control). SCp2 transduced with FL-MMP3 had the highest invasive rate, followed by EA and dPEX-SCp2, respectively (Fig. 1H). These data indicate that despite the background proteolytic activity, MMP3 requires the hemopexin domain to induce invasion in SCp2 cells. A similar trend was obtained with EpH4, another mouse mammary epithelial cell line (Supplemental Fig. S2B–E).

Proteomic screen identifies HSP90β as interacting with the hemopexin domain of MMP3

Because MMP3 is a secreted protein, we asked whether the secreted form of this enzyme and its mutants were required to induce the morphological and functional changes observed (Supplemental Fig. S3). Conditioned medium (CM) from FL-SCp2 was sufficient to induce scattering, elongated shape, and a substantial increase in invasion in parental SCp2 cells. Whereas dPEX-SCp2 CM did not trigger scattering or enhance the elliptical factor, there was a small but significant increase in invasion. However, when the proteolytic activity of the MMP3 construct was ablated (CM from EA-SCp2), there was still
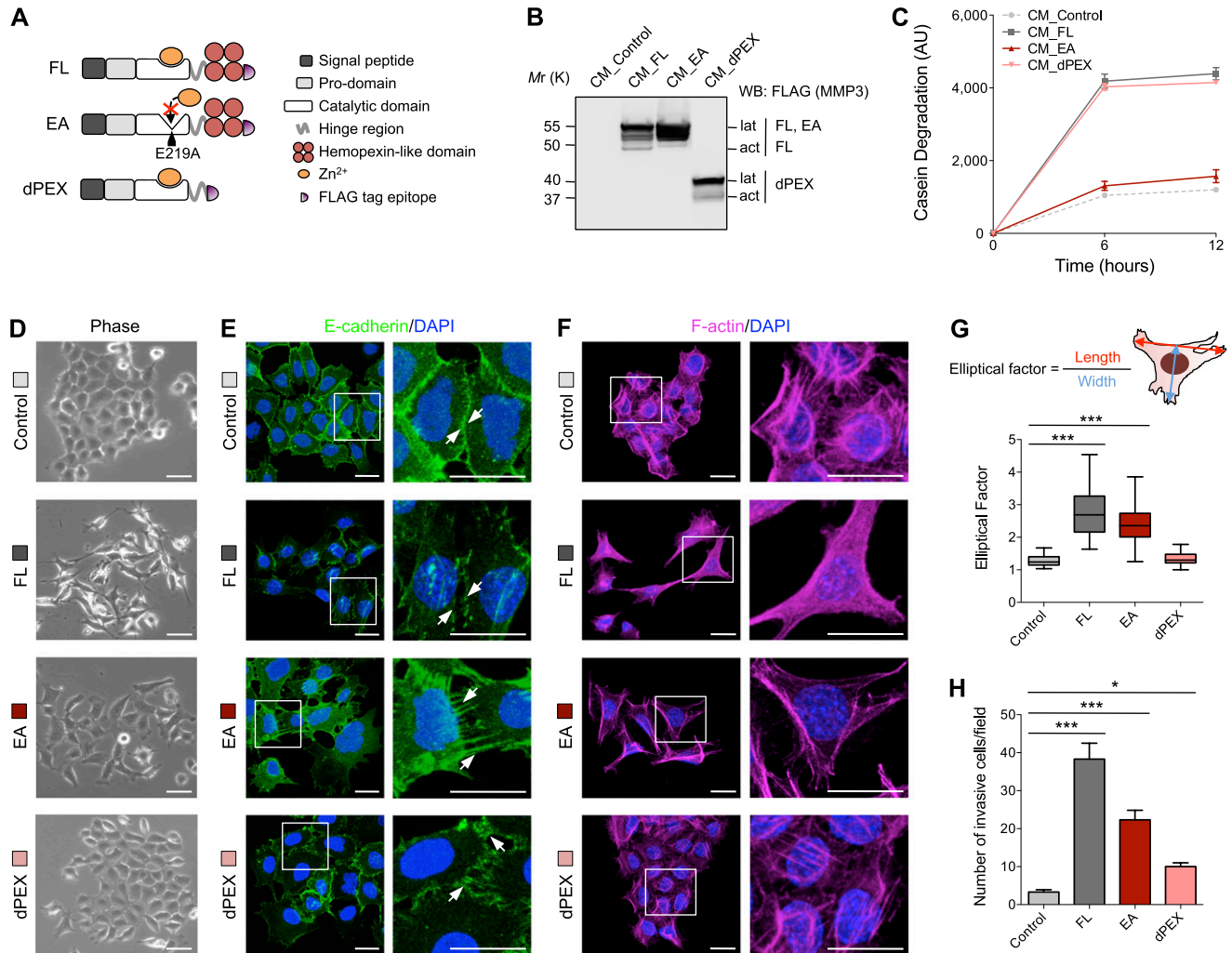
Figure 1. The MMP3 hemopexin domain induces altered morphology and invasion in mammary epithelial cells. (*A*) Schematic representation of engineered constructs: the full-length MMP3 (FL) and two mutants (EA and dPEX). (*B*) Overexpression of MMP3 and its mutants in SCp2 cells assessed by Western blotting (WB). CM was isolated from cells transduced with each of the MMP3 constructs and the control vector. Flag epitope tag was detected with anti-Flag antibody. Both latent (lat) and activated (act) forms of MMP3 were recognized. (*C*) MMP3 proteolytic activity of SCp2 cells overexpressing each construct assayed by casein degradation. CM was incubated with a dye-quenching casein substrate (BODIPY TR-X casein). MMP3-mediated degradation of casein generated fluorescent dye-labeled peptides that were monitored over time. Fluorescence intensity is indicated as arbitrary units (AU). (*D*) Overexpression of MMP3 containing the hemopexin domain induces scattering in SCp2 cells. Scattering ability was evaluated in cells transduced with each construct upon stimulation with epidermal growth factor (EGF). Bars, 20 μm. (*E*) The presence of the hemopexin domain of MMP3 is required to disrupt adherens junctions. Immunofluorescence images show E-cadherin distribution (green) in cells expressing each construct. Arrows depict areas of cell–cell contact. Nuclei were stained with DAPI (blue). Bars, 10 μm. (*F*) The MMP3 hemopexin domain induces reorganization of F-actin. Images show F-actin (magenta) and nuclei (DAPI; blue) in each culture. Bars, 10 μm. (*G*) Quantification of morphological changes in each culture by calculation of the cellular elliptical factor. This is defined as the ratio of the longest (length) to the shortest (width) axis of the cell. The box plot shows the median and the interquartile range, and the whiskers show the extreme values. $n = 100$ cells for each stable cell line. (***) $P < 0.0001$ by Student's *t*-test. (*H*) The MMP3 hemopexin domain is required for invasion. Invasiveness in each condition was assayed in Boyden chambers. Results are indicated as mean ± SD from three independent experiments (10 bright-field images in 20× magnification were counted). (***) $P < 0.0001$; (*) $P < 0.05$ by Student's *t*-test.

a considerable increase in invasion, and cells were elongated. This finding additionally supports the fact that the hemopexin domain is required for invasion in SCp2 cells and raises the question of whether MMP3 functions alone or depends on other factors being present in CM. The hemopexin domain of MMPs is known to interact with other proteins. The MMP14 hemopexin domain was reported to be required for invasion through Col-1 (Tam et al. 2002; Wang et al. 2004) and for binding to the adhesion receptor CD44 and integrin-β1 (Mori et al. 2002, 2013).

To explore what other factors may be required for the functional activities of MMP3, we isolated Flag-tagged FL

or dPEX protein complexes from CM and performed a proteomic analysis to identify proteins that interact with the MMP3 hemopexin domain (Fig. 2A). Based on spectra counts, we selected proteins with abundances >1.5-fold change in FL compared with dPEX (Fig. 2B, left;

Supplemental Fig. S4). Amongst the 75 proteins that passed the selection criteria, we selected myristoylated alanine-rich C-kinase substrate (MARCKS) and annexin A2 (ANXA2), which were previously implicated in regulation of cell shape, motility, and invasion in *Xenopus*
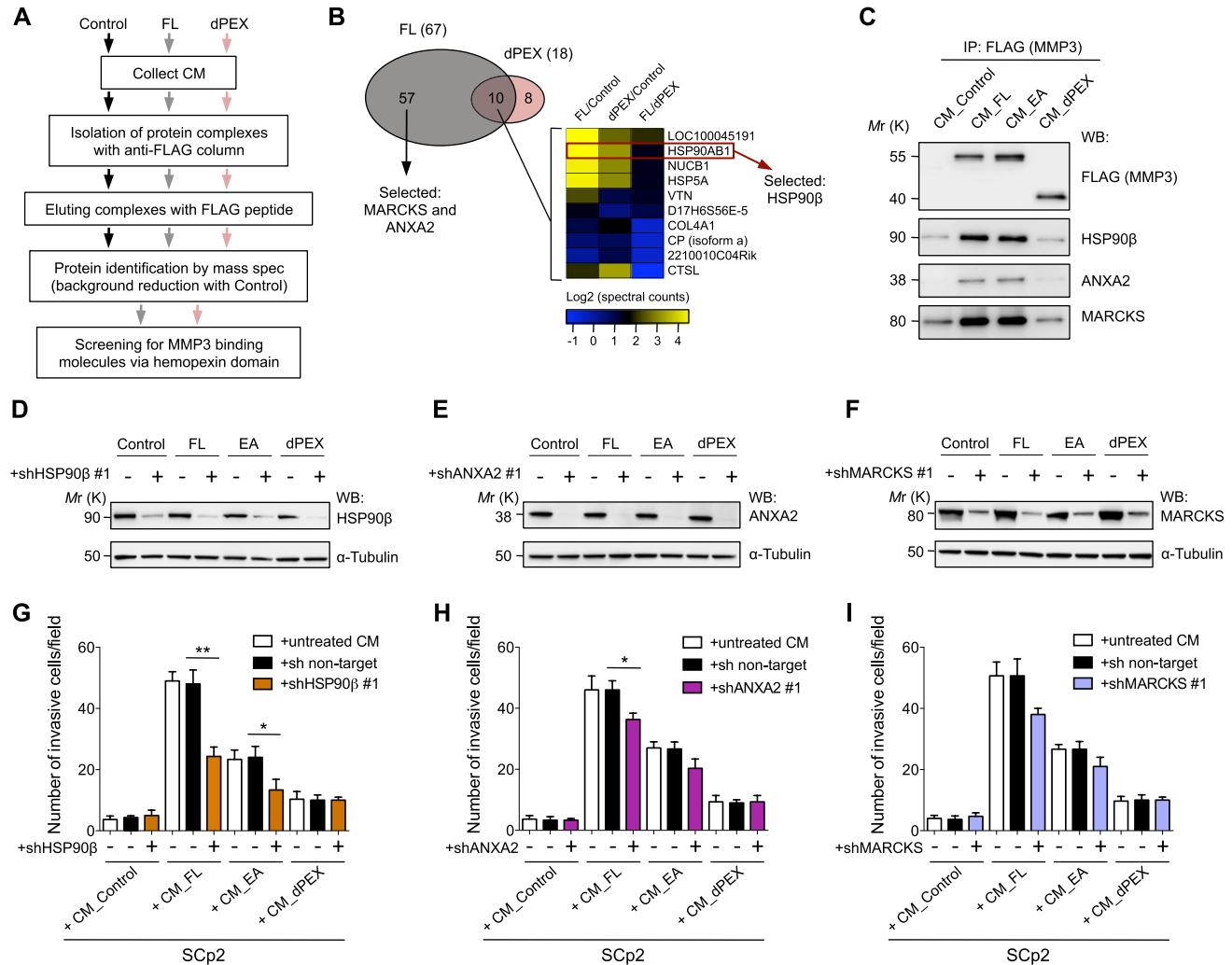
Figure 2. Proteomic screen of MMP3-binding partners reveals an extracellular role for HSP90β, ANXA2, and MARCKS in MMP3-driven invasion via the hemopexin domain. (*A*) Strategy for screening MMP3-binding partners through the hemopexin domain. (*B*) Selection of MARCKS, ANXA2, and HSP90β from proteomic analysis. (*Left*) Venn diagram showing the spectrum of proteins detected in FL and/or dPEX Flag-immunoprecipitated samples. (*Right*) Heat map illustrating the relative difference in abundance of proteins detected in both FL and dPEX but much higher in FL. Proteins were sorted by the highest ratio between FL and dPEX. (*C*) Co-IP of each mutant shows the association between MMP3 and the selected targets via the hemopexin domain. Flag-tagged MMP3 FL, EA, and dPEX were immunoprecipitated from CM with an anti-Flag antibody and blotted with antibodies for its binding partners. (*D–F*) Blots showing shRNA-mediated silencing of HSP90β (*D*), ANXA2 (*E*), and MARCKS (*F*) in SCp2 cells overexpressing each of the MMP3 constructs and the control vector. Knockdowns were reproduced using two other shRNAs for each one of the targets (Supplemental Fig. S5A–C,G–I). Nontargeting shRNA was used as negative control. Knockdowns were verified by Western blotting of whole-cell lysates with antibodies specific for each target protein. α-Tubulin was used as loading control. (*G–I*) Silencing of HSP90β, ANXA2, and MARCKS reduces MMP3-driven invasion in SCp2 cells when the hemopexin domain of MMP3 is present. SCp2 cells were cotransduced with each of the MMP3 constructs and either nontargeting shRNA or shRNAs selectively targeting HSP90β (*G*), ANXA2 (*H*), or MARCKS (*I*). SCp2 parental cells were treated with CM from each engineered cell line and assayed for invasiveness in Boyden chambers. Parental cells treated with CM from SCp2 cells expressing each of the MMP3 constructs and the control vector (untreated CM) were used as control. Results are expressed as mean ± SD from three independent experiments (10 bright-field images in 20× magnification were counted in each experiment). (**) $P < 0.001$; (*) $P < 0.05$ by Student's *t*-test. The biological effects of shRNA-mediated knockdowns were reproduced with two other shRNAs for each of the three interacting proteins (Supplemental Fig. S5D–F,J–L).

embryos and canine kidney cells (Iioka et al. 2004; de Graauw et al. 2008). Additionally, we selected HSP90β, detected in both FL and dPEX but much higher in FL (Fig. 2B, right). We validated the interaction of the hemopexin domain of MMP3 with these three proteins by coimmunoprecipitation (co-IP) (Fig. 2C).

We then asked whether this interaction is functionally significant and required for MMP3-induced invasion. We generated SCp2 cell lines coexpressing each of the MMP3 constructs and either nontargeting shRNA (negative control) or shRNA selectively targeting each of the three proteins (Fig. 2D–F). We treated parental SCp2 with CM from each engineered cell line and screened for invasion using Boyden chambers (Fig. 2G–I). Whereas the knockdown did not affect invasion of cells treated with CM from control or dPEX-SCp2, it significantly reduced the invasiveness of cells treated with FL or EA-SCp2 CM. These results indicate that binding of each one of these three proteins to the hemopexin domain of MMP3 has functional significance, but the inhibition was much more dramatic when HSP90β was inhibited (Fig. 2G). The nature of the complexes containing MMP3 and HSP90β was clarified further by reverse co-IP of HSP90β protein complexes from CM of control SCp2 cells (Supplemental Fig. S6). Whereas the association of MMP3 and HSP90β was confirmed in reverse, ANXA2 and MARCKS could not be recovered in the immunoprecipitated fraction under these conditions. This suggests that either these proteins do not exist in a single complex at a given time—but may instead represent a network of proteins interacting with one another at different times for different purposes—or the interaction of the other two proteins is weak and thus cannot be detected easily by the reverse co-IP. These data also justify the importance of HSP90β as the major player in regulation of MMP3 function.

The levels of extracellular HSP90β determine MMP3-induced invasion

Given the significance of HSP90β in cellular and tissue function, we concentrated on understanding the role of this molecule in regulating MMP3. The levels of HSP90β in each engineered cell line were tuned by adding either a recombinant protein or a specific inhibitor (CCT018159) (Sharp et al. 2007). Increasing HSP90β levels enhanced invasion significantly in FL and EA-SCp2 (Supplemental Fig. S7A, second and third panels) but did not raise the invasive potential of dPEX-SCp2 or control cells significantly (Supplemental Figure S7A, first and last panels). Conversely, inhibition of HSP90β reduced invasion in FL and EA-SCp2 (Supplemental Fig. S7B, second and third panels) and had no significant effect on dPEX-SCp2 or control cells (Supplemental Figure S7B, first and last panels). The above pattern was reproduced when we used a function-blocking antibody against HSP90β and demonstrated that inhibition of extracellular HSP90β was sufficient to reduce invasiveness of FL and EA-SCp2 (Supplemental Fig. S7C). These data show that MMP3 is unable to perform much of its invasive functions without interacting with HSP90β in the extracellular milieu.

The hemopexin domain is required for the invasive function of MMP3 during branching morphogenesis

The finding of the critical role of the hemopexin domain in the invasion function of MMP3 in cell lines needed to be confirmed in a more physiological context. We used two culture models that simulate the normal processes of mammary invasion and branching: primary mammary organoids (Fig. 3A; Simian et al. 2001) and cell clusters of a functionally normal mouse mammary epithelial cell line (EpH4) (Supplemental Fig. S8A; Hirai et al. 1998; Mori et al. 2013) embedded in Col-1 gels. The physiological relevance of this model is illustrated by the presence of copious amounts of Col-1 in the stroma surrounding epithelial ducts in the murine mammary gland (Williams and Daniel 1983).

There are a number of advantages of using the versatile assay using organoids from the mammary gland. Cell–cell and cell–matrix interactions remain intact, and the architecture of the tissue is not disrupted. Additionally, we can prepare enough mammary organoids from a single mouse (~1200) and infect with the four distinct constructs. Even inbred mice are known to change biochemical and morphological characteristics at different stages of the estrogen cycle as well as in response to handling and context. In this way, we could control for all variations and avoid the excessive use of animals but also achieve statistical significance. Last, we could mark them: The presence of the GFP in the constructs indicated that >80% of the cells were infected. These cultures allow us to not only create a physiological condition where the organoids regenerate an epithelial tree-like structure, but also observe and control extracellular events much more robustly.

The functional significance of the hemopexin domain was reproduced in our three-dimensional (3D) assays with clustered EpH4 cells (Supplemental Fig. S8B) and, most importantly, with primary organoids (Fig. 3B). We used two different criteria to quantify invasion and branching of organoids: the number of extended sprouts and processes developed from each structure (Fig. 3C) and the spatial network per organoid (Fig. 3D). As expected, organoids overexpressing FL-MMP3 had the highest number of extending processes and the longest spatial network, indicating that the proteolytic activity would still be necessary if the path is obstructed.

For the purpose of the current experiments, we did not distinguish between branches that were more than one cell layer thick and demonstrated basal and apical polarity and strands that grew as a single file. However, there were very few of the latter in dPEX-overexpressing and control cultures. As mentioned above, we advisedly decided against inhibiting the endogenous MMP3 activity using multiple genetic manipulations because both cells and organoids were sensitive to more than one set of viral infections. We therefore used a peptide that has been shown to inhibit MMP3 proteolytic activity effectively and specifically (Fotouhi et al. 1994; Farina et al. 2002). Inhibition of both endogenous and exogenous MMP3 proteolytic activity decreased branches in a dose-dependent manner in all organoids (Supplemental Fig. S9). Nevertheless,
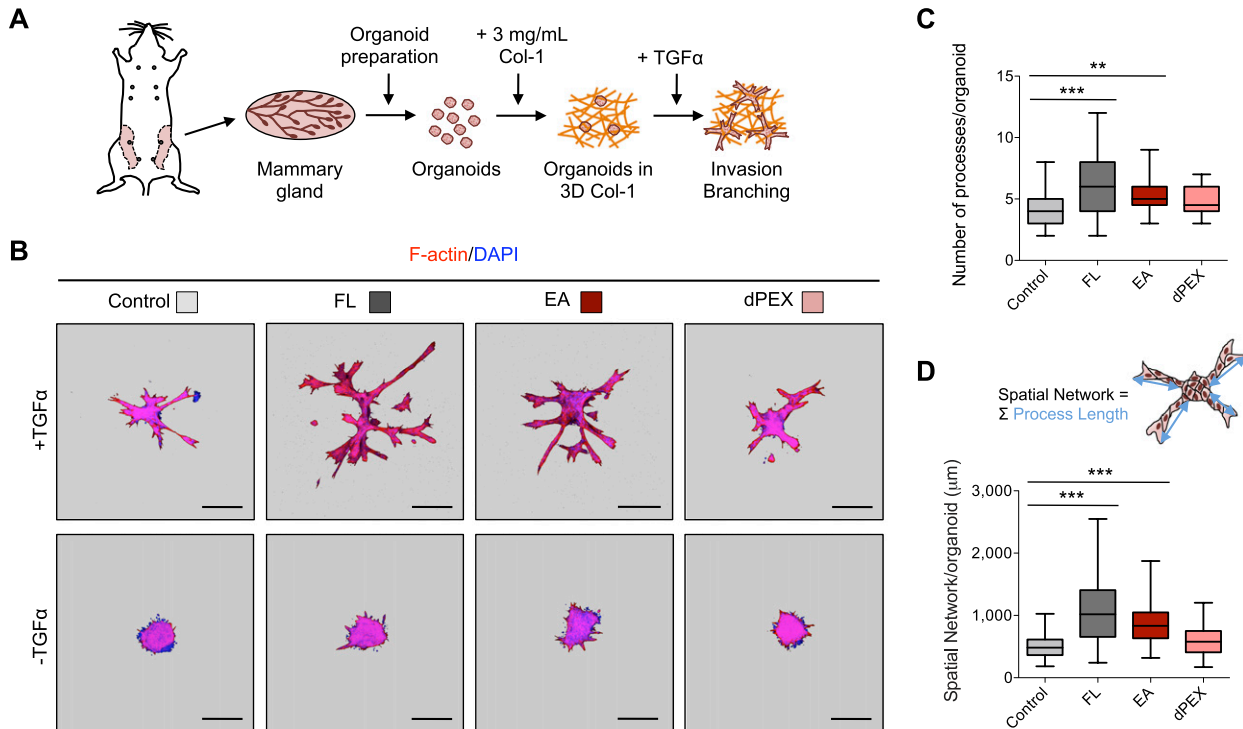
Figure 3. The hemopexin domain of MMP3 is necessary to direct the epithelial invasion of mammary organoids in 3D Col-1 gels even without the proteolytic activity. (A) Schematic representation of primary mammary organoid preparation and culture in 3D Col-1 gels. (B) Overexpression of MMP3 containing the hemopexin domain enhances the invasion of mammary organoids in Col-1. Images of maximum intensity projection of mammary organoids transduced with each of the MMP3 constructs as well as the control vector and cultured in 3 mg/mL Col-1 gels for 3 d. Organoids invaded and branched only in the presence of the growth factor (TGFα). Structures were stained for F-actin (red) and nuclei (DAPI; blue). Image background was pseudo-colored in gray. Bars, 100 μm. (C) The presence of the hemopexin domain of MMP3 increases the number of extending processes developed from each organoid invading through Col-1 (150 organoids were counted per culture). (***) $P < 0.0001$; (**) $P < 0.001$ by Student's t-test. (D) The size of the spatial network per organoid is increased by overexpression of MMP3 containing the hemopexin domain. The spatial network per organoid is defined as the sum of the length of all the extending processes of an organoid (50 organoids were counted per culture). (***) $P < 0.0001$ by Student's t-test.

there still was invasion of cells individually or in a single file, with less branching than untreated cultures (Supplemental Fig. S9A). These data indicate that the hemopexin domain of MMP3 allows epithelial invasion, but in the presence of proteolytic activity, there are more multilayered branches. Additionally, when we knocked down MMP3 in control organoids, there was a significant decrease in invasion and branching (Supplemental Fig. S10). This reaffirms the requirement for MMP3 for mammary branching morphogenesis and provides an additional reason for our choice of preserving the endogenous MMP3 intact.

The interaction of HSP90β with MMP3 is required for invasion

Having shown the relevance of the distinct domains for invasion and branching also in organoids, we examined the requirement of HSP90β in organoids transduced with different constructs receiving either recombinant protein (Fig. 4A) or a function-blocking antibody against HSP90β (Fig. 4B). The recombinant HSP90β added extracellularly enabled the secreted MMP3 to induce the most exuberant branched structures (Fig. 4A, bottom right) and the longest

spatial network observed so far (Fig. 4C, right). Importantly, blocking the extracellular HSP90β with inhibitory antibodies added to the medium abolished branching ability in all organoids, including controls (Fig. 4B [bottom], D). Organoids receiving the construct with a deleted hemopexin domain were essentially identical to the controls. Additionally, there was very little co-IP of MMP3 with HSP90β in the absence of exogenous HSP90β (data not shown). These findings identify the crucial role of extracellular HSP90β in mammary epithelial invasion and branching, with binding occurring in the presence of the hemopexin domain of MMP3.

Discussion

The importance of MMPs for sculpting the architecture of branched organs is well accepted. This statement is demonstrated in particular in the mammary gland. We and others showed that overexpression of MMP3 in mammary epithelia enhanced lateral branching and precocious alveolar development in virgin mice (Sympson et al. 1994; Witty et al. 1995). These mice eventually developed tumors that exhibited chromosomal aberrations (Sternlicht et al.
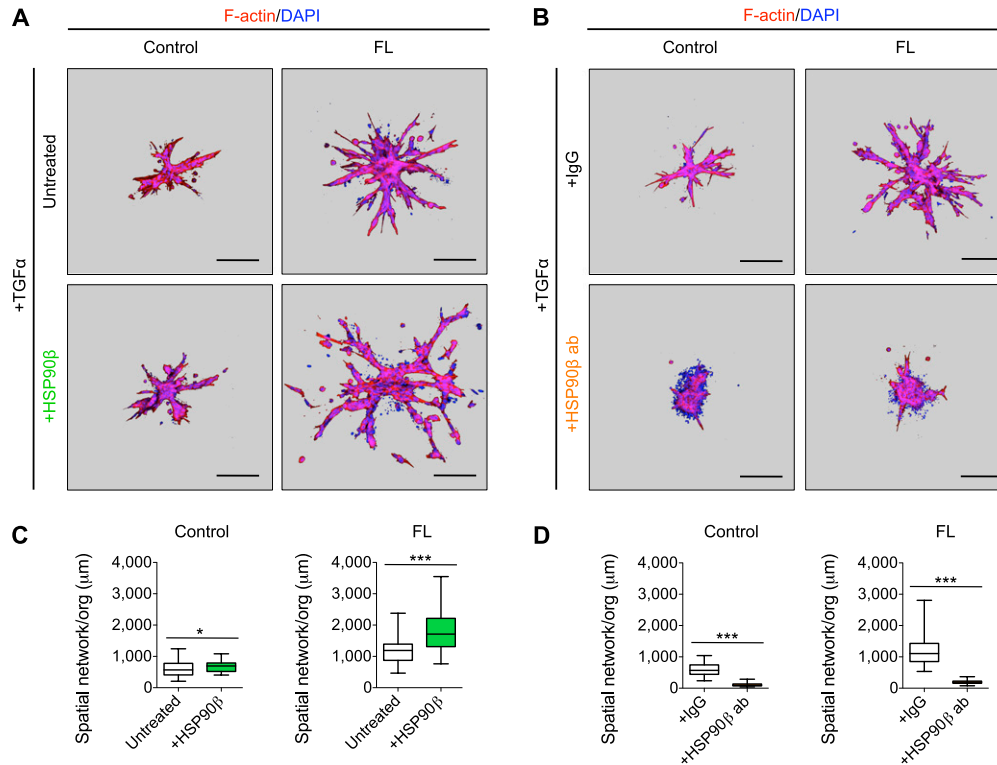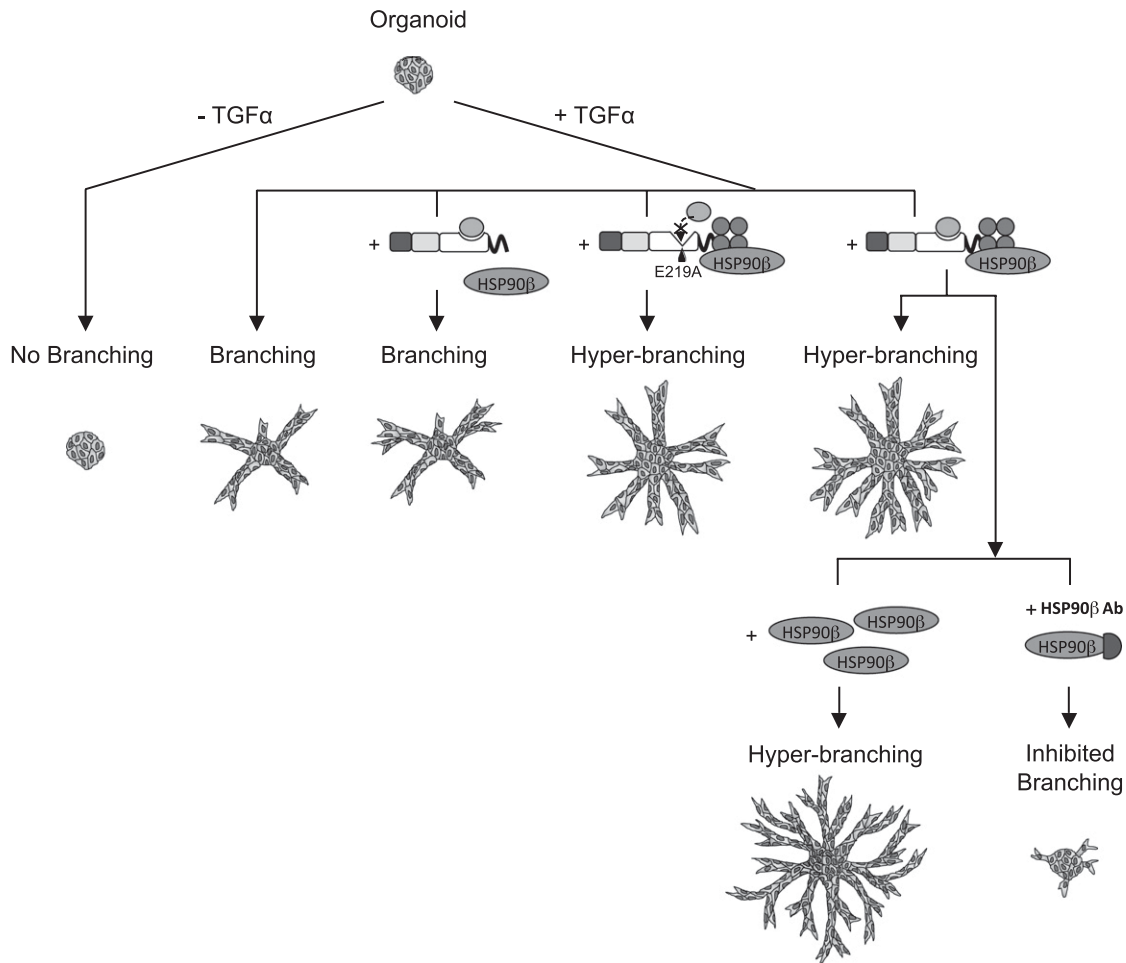
Figure 4. Extracellular HSP90β modulates MMP3 function in invasion and branching of mammary epithelial organoids. (*A*) Recombinant HSP90β added to the medium increases the invasiveness of mammary organoids expressing MMP3. Images of maximum intensity projection from confocal z-stacks of mammary organoids overexpressing FL-MMP3 or control vector embedded in 3 mg/mL Col-1 gels. Organoids were cultured for 3 d in the presence or absence of a recombinant HSP90β. Structures were stained for F-actin (red) and nuclei (DAPI; blue). Image background was pseudo-colored in gray. Bars, 100 μm. (*B*) Inhibition of extracellular HSP90β abolishes the branching ability of mammary organoids. Images of maximum intensity projection from confocal z-stacks of mammary organoids overexpressing FL MMP3 or control vector embedded in 3 mg/mL Col-1 gels. Organoids were cultured for 3 d with a function-blocking antibody against HSP90β or a control IgG. Structures were stained for F-actin (red) and nuclei (DAPI; blue). Image background was pseudo-colored in gray. Bars, 100 μm. (*C,D*) Quantification of invasion and branching by measuring the spatial network per organoid (50 organoids were counted per culture). (***) $P < 0.0001$; (*) $P < 0.05$ by Student's *t*-test.

1999) through a mechanism dependent on ROS and RAC1B, a spliced variant of RAC1 (Radisky et al. 2005). Conversely, we showed that MMP3 controls lateral branching in vivo (Wiseman et al. 2003) and in Col-1 gels (Simian et al. 2001).

In many of these experiments, we and others had assumed that the catalytic domain of MMP3 was responsible for these functions. More recently, there has been some biochemical evidence that the hemopexin domain of some MMPs has a role in the nonproteolytic function. Mori et al. (2002) and Dufour et al. (2008) examined the role of the hemopexin domain of MMP14 and MMP9 in cancer cells and fibroblasts, respectively, and showed that it is necessary for cell migration. Likewise, the hemopexin domain, but not the catalytic activity, of MMP12 was shown to be required for the antimicrobial function of this enzyme (Houghton et al. 2009). The only clear evidence for the physiological relevance of the hemopexin domain in vivo came from a report by Glasheen et al. (2009) in *Drosophila*; these investigations showed that whereas the catalytic domain was still required for all MMP functions, the hemopexin domain was specifically implicated in invasion during metamorphosis.

Neither the requirement for the hemopexin domain of MMP3 nor the surprising interaction with extracellular HSP90β were known or reported previously. Here we show that cells and tissues that overexpress MMP3 but lack catalytic activity can invade and branch easily in 3D Col-1 gels. Additionally and importantly, we show that the functional activity of the hemopexin domain of MMP3 requires extracellular interaction with HSP90β (Fig. 5).

The previous literature on functions of HSP90 place its activity essentially within the cell, where it works as a "hub of protein homeostasis" by facilitating the maturation of a wide range of proteins (Taipale et al. 2010). It is only with regard to HSP90α that the extracellular function has been mentioned. A number of investigators have shown that the α isoform of HSP90 is present in CM of either cancer cells or "wounded cultures" (Eustace et al. 2004; Li et al. 2007; Cheng et al. 2008). Our discovery that the extracellular HSP90β is essential for MMP3-driven invasion and branching adds a new dimension to this chaperone's functions. Despite the fact that HSP90α and HSP70, which was shown previously to increase the association between MMP2 and HSP90α in vitro (Sims

Figure 5. Scheme of the essential role of extracellular HSP90β in the modulation of MMP3-driven invasion and branching in mammary organoids. When organoids from the mammary gland are embedded within 3D gels of Col-1, they undergo invasion and branching morphogenesis upon addition of growth factors. The small endogenous MMP3 activity present in the organoids provides them a baseline of branching to which we could compare the exogenous constructs. The insertion of exogenous MMP3 induces a hyperbranched phenotype only when the hemopexin domain is present. This region mediates the extracellular interaction with HSP90β and is critical for the invasive function of MMP3. Recombinant HSP90β added extracellularly enables the secreted MMP3 to induce the most exuberant branched structures. Conversely, blocking of extracellular HSP90β with inhibitory antibodies added to the medium abolishes branching ability.

et al. 2011), are present intracellularly in our model, they are not found in the extracellular milieu (data not shown). That HSP90β has a crucial extracellular function was shown by addition of specific inhibitory antibodies to the medium, resulting in complete inhibition of branching (Fig. 4B,D). These data indicate that the presence of HSP90β in the medium is a selective process and is not due to cell lysis or apoptosis.

Mice deficient for HSP90β fail to develop a placental labyrinth and die around mid-gestation (Voss et al. 2000). This fact prevented us from characterizing their mammary gland development in vivo. Additionally, despite the fact that *Mmp3*-null mice are viable and fertile, they compensate the reduced secondary and tertiary branching phenotype by day 70 (Wiseman et al. 2003). The use of ECM gels, however, has allowed us to elucidate the role of different domains of MMP3 as well as prove that extracellular HSP90β regulates MMP3 function in invasion and branching through interaction with the hemopexin domain. The primary organoids develop into hundreds of minimammary epithelial trees, thus offering a model of mammary epithelial development in a robust and manipulable format.

The signaling pathways and regulatory mechanisms that drive branching in mammalian organs have been described by a number of laboratories, including ours, and involve multiple members of the receptor tyrosine kinase (RTK) family (for review, see Lu and Werb 2008). Sustained activation of MAPK$^{ERK-1,2}$ in response to hepatocyte growth factor was shown to be required for kidney epithelial morphogenesis in Col-1 gels (Maroun et al. 2000). We showed that the MAPK$^{ERK-1,2}$ pathway also integrates distinct and antagonistic signals from TGFα and FGF7 to determine the final morphogenetic response of mammary organoids cultured in lrECM; sustained MAPK activation downstream from TGFα and EGFR in-

duces branching, whereas its transient activation downstream from FGF7 and FGFR2 stimulates proliferation but not branching (Fata et al. 2007). FGF7 acts in part by suppressing the expression of MMP3, and inhibition of the latter reduces branching significantly both in culture and in vivo (Simian et al. 2001; Wiseman et al. 2003). Our discovery that extracellular HSP90β is critical for MMP3 function in invasion and branching places HSP90β as an important player in the signaling pathways that determine the final mammary morphogenetic fate.

The presence of HSP90 in murine mammary glands was reported in 1989 (Catelli et al. 1989); therefore, it is surprising that its role in functional and morphogenetic aspects of the mammary gland is still poorly understood. The fact that HSPs have been postulated as molecular chaperones that mitigate the life-threatening effects of heat and other stresses on the proteome (Taipale et al. 2010) poses the question of whether HSP90β may also play a role in stabilization and maturation of MMP3. We are now beginning to understand that HSP90's functions extend well beyond stress tolerance, and associated changes in its clients can then exert marked effects on the relationship between genotype and phenotype, influencing human health, disease, and evolutionary processes (Rutherford and Lindquist 1998; Queitsch et al. 2002; Cowen and Lindquist 2005). The presence of HSP90β in the medium and the functional significance of its interaction with MMP3 are further proof that HSP90-mediated events are above and beyond the heat-shock response. Our preliminary data indicate that the extracellular source of HSP90β for luminal epithelial branching most probably is the myoepithelial cells in vivo (data not shown). These data, combined with some evidence that MMP3 is mainly produced by stromal fibroblasts (Witty et al. 1995; Kouros-Mehr and Werb 2006), raise the exciting possibility that extracellular interaction of HSP90β with MMP3 may be a way for different cell types to communicate in the coordination of the normal processes of invasion and branching.

In the initial mass spectrometry data, we found many additional molecules that appear to be interacting with MMP3. In particular, we show that ANXA2 and MARCKS were coimmunoprecipitated with MMP3, with binding occurring in the presence of the hemopexin domain. Our preliminary data also showed that depletion of each of these proteins reduced invasiveness in SCp2 cells. Unlike the interaction between HSP90β and MMP3 that happened in both directions, the reverse co-IP of ANXA2 and MARCKS with HSP90β could not be confirmed under these conditions. In addition, our proteomic screen identified other proteases such as ADAM10, ADAMTS15, and Cathepsins A and L as possible proteins that may interact extracellularly with MMP3 (Supplemental Fig. S4). The functional significance of these latter proteins remains to be determined. Our data from the mass spectrometry, however, tentatively suggest that a cascade of proteases might function collectively to orchestrate epithelial invasion.

Finally, we showed most recently that the signaling module for MMP14, a membrane-bound MMP, in branching of the end bud of the mammary gland of virgin mice is its transmembrane/cytoplasmic domain in conjunction with integrin-β1 (Mori et al. 2013). Thus, the findings presented here, along with the above work, may provide a compelling explanation for why inhibitors of MMPs failed so dramatically in the clinic (Overall and Kleifeld 2006). Targeting noncatalytic sites of MMPs as well as the interacting partners with agents such as small inhibitors or antibodies for the binding sites of integrin-β1 and HSP90β may yield more effective and tissue-specific inhibitors.

Materials and methods

Restriction enzymes, antibodies, proteins, and chemical reagents

All restriction enzymes were acquired from New England Biolabs. Bovine dermis acid-solubilized Col-1 solution (IAC-50) was purchased from Koken. Antibodies against the following proteins were obtained as indicated: Flag (F1804, M2, Sigma; 1:500 for Western blotting), E-cadherin (13-1900, clone ECCD-2, Invitrogen; 1:1000 for Western blotting; 1:200 for immunofluorescence), HSP90β (5087, Cell Signaling, 1:1000 for Western blotting), HSP90β (NBP1-61773, Novus Biologicals; 40 µg/mL for function-blocking experiments; 10 µg for co-IP experiments), MARCKS (P0370, Sigma; 1:1000 for Western blotting), ANXA2 (AF3928, R&D Systems; 1:1000 for Western blotting), MMP3 (ab18898, Abcam; 1:1000 for Western blotting), α-tubulin (T6074, clone B-5-1-2, Sigma; 1:5000 for Western blotting), and rabbit IgG (2729, Cell Signaling; 40 µg/mL for function-blocking experiments). Alexa Fluor 594 Phalloidin (A12381, Molecular Probes; 1:400) was used to stain F-actin. DAPI (Sigma) was used to stain nuclei. HSP90β inhibitor CCT018159 (385920), MMP3-specific peptide-based inhibitor (444218), and recombinant HSP90β (385903) were purchased from Calbiochem/EMD Millipore.

Construction of expression plasmids

All MMP3 mutants were constructed using a PCR-based method (details in the Supplemental Material). The cDNA sequence used as a template was cloned from a human breast cell line and sequence-confirmed by comparison with gene accession number NM_002422.3. FL contains the full-length MMP3 cDNA. EA is a catalytically inactive mutant, holding a point mutation E219A at the catalytic core. dPEX is a hemopexin-like domain-deleted mutant (ΔN289-C477). A mammalian expression vector, pCDH-EF1-MCS-T2A-copGFP (System Biosciences), was used to express the gene products. To detect MMP3 protein, the Flag epitope (Asp–Tyr–Lys–Asp–Asp–Asp–Asp–Lys) was inserted at the C terminus of every construct generated. All cDNA constructs were confirmed by DNA sequencing.

shRNA-mediated knockdowns

shRNA constructs selectively targeting HSP90β, ANXA2, MARCKS, or MMP3 were purchased from MISSION shRNA library (Sigma) (sequences are detailed in Supplemental Table S1). Control cells were infected with nontargeting shRNA (SHC002, Sigma). Knockdown efficiency was verified by Western blotting with the appropriate antibodies.

Cell culture and transduction

SCp2 cells were cultured in Dulbecco's modified Eagle's medium/Ham's F-12 nutrient mixture (DMEM/F-12) supplemented with 5% fetal bovine serum (FBS), 5 µg/mL insulin, and 50 µg/mL

gentamicin and maintained as previously described (Desprez et al. 1993). EpH4 cells were cultured in DMEM/F-12 medium supplemented with 2% FBS, 5 μg/mL insulin, and 50 μg/mL gentamicin and maintained as previously described (Reichmann et al. 1989). For transduction, cells were seeded in 24-well plates (1×10^5 cells per well) and infected with lentiviral particles carrying different expression plasmids using MISSION ExpressMag Beads (Sigma) according to the manufacturer's instructions. Cells transduced with lentivirus carrying shRNA constructs were additionally selected with 2 μg/mL puromycin.

Preparation of primary mammary organoids and transduction

Primary epithelial organoids were isolated from 8-wk-old virgin FVB mice as previously described (Fata et al. 2007). Briefly, inguinal glands were removed, minced with two parallel razor blades, and gently shaken for 30 min at 37°C in a 50-mL collagenase/trypsin mixture (0.2% trypsin, 0.2% type-IV collagenase, 5% FBS, 5 μg/mL insulin in DMEM/F-12). After centrifugation at 80g for 10 min, supernatant was discarded, and the cell pellet was resuspended in DMEM/F-12. The suspension was pelleted again, resuspended in 4 mL of DMEM/F-12 containing 80 U of DNase I (Sigma), and incubated for 5 min at room temperature with occasional shaking. After the suspension was spun at 80g for 10 min, a series of differential centrifugations in DMEM/F-12 was implemented to separate the epithelial organoids from single cells, fibroblasts, and fibrillar extracellular matrices. The final pellet was resuspended in the desired amount of medium. For transduction, organoids were seeded in 24-well polyhema-coated plates (1000 organoids per well) and infected with lentivirus in the presence of 8 μg/mL polybrene for 24 h.

Preparation of cell clusters and transduction

EpH4 cells suspended in growth medium were plated in six-well polyhema-coated plates (1×10^5 cells per well) and incubated overnight at 37°C, yielding rounded clusters. Single cells were removed by differential centrifugation, and the final pellet was resuspended in the desired amount of medium.

Branching morphogenesis assay

Primary organoids or clustered EpH4 cells were embedded in 3D Col-1 gels as previously published (Simian et al. 2001; Mori et al. 2013). In brief, acid-solubilized Col-1 solution was mixed gently on ice with 1 vol of 10× DMEM/F-12 (pH adjusted to 7.4 with 0.1 M NaOH), and the concentration was adjusted to 3 mg/mL with DMEM/F-12. A basal layer of 80 μL of Col-1 was poured into each well of an eight-well chambered coverglass (155409, Thermo Scientific) and allowed to gel for 5 min at 37°C. A second layer of 200 μL of Col-1 containing 150 organoids or EpH4 clusters was added to each well and placed immediately at 37°C. After gelation, 400 μL of chemically defined medium (DMEM/F-12 containing 1% insulin/transferrin/selenium, 1% penicilin/streptomycin) with 9 nM TGFα (Sigma) or 9 nM bFGF (Sigma) was added to each well (unless stated otherwise) and replaced every other day.

After 3 d of culture, gels were fixed with 4% formalin for 30 min and stained with phalloidin and DAPI for 1 h. Structures were imaged with an upright Zeiss LSM710 using a 0.8 NA 20× air objective. An organoid or cell cluster was defined as invading and branching when it had at least three independent extending processes that were at least half the diameter of the center of the organoid or cell cluster. The number of extending processes and their average length were determined using the Imaris program (Bitplane). We defined a new metric of invasion and branching,

which we refer to as the spatial network per organoid. This is defined as the sum of the length of all of the extending processes developed from each organoid. Fifty structures were counted per condition, and the experiments were executed at least three times.

Caseinase activity assay

CM was incubated with a casein derivative-quenching red-fluorescent dye (BODIPY TR-X Casein, E6639, Invitrogen). Protease-catalyzed hydrolysis released highly fluorescent BODIPY TR-X dye-labeled peptides. The accompanying increase in fluorescence is proportional to MMP3 proteolytic activity and was monitored with a microplate reader. A control without BODIPY casein was used to subtract residual fluorescence background.

Cell scatter assay

SCp2 cells were seeded in six-well plates at low density (1×10^5 cells per well), allowed to form colonies (~48 h), and serum-starved for 24 h. Epithelial cell islets were then stimulated with 9 nM epidermal growth factor (EGF) (Sigma) and imaged at 48 h with a Zeiss Imager Z1 microscope using a 10× objective.

Immunofluorescence

SCp2 cells were cultured for 72 h on glass coverslips, fixed with 4% paraformaldehyde/PBS for 10 min, washed with PBS, and permeabilized in 0.25% Triton X-100/PBS for 10 min. Samples were blocked with 1% BSA and 5% goat serum/PBS for 1 h, followed by incubation with the primary antibody in blocking buffer overnight at 4°C and the secondary antibody for 1 h at room temperature. Images were acquired with an upright Zeiss LSM710 using a 1.4 NA 63× oil immersion.

Morphometry analysis

Cell edges were outlined in F-actin-stained cells using an "Object Identification Module" from CellProfiler software (Carpenter et al. 2006). Cellular elliptical factors, defined as the ratio of the longest (length) to the shortest (width) axis of the cell, were calculated for 100 random cells per culture.

Invasion assay

Cell culture inserts (8 μm, 24-well format; BD Biosciences) were evenly coated with 20 μL of diluted (1:5 in DMEM/F-12 medium) Matrigel (BD Biosciences). Cells (1×10^5) in 200 μL of DMEM/F-12 medium or different CM (as indicated in each experiment) were added to the upper compartment of the chamber. The lower compartment of the chamber was filled with 300 μL of medium containing 10% FBS as a chemoattractant. After 48 h of incubation at 37°C, the top side of the insert was cleared from noninvasive cells with a cotton swab and washed with serum-free DMEM/F-12. The remaining (invasive) cells at the lower surface of the filter were fixed and stained with a solution of Coomassie Blue 0.125% in methanol:acetic acid:H_2O (45%:10%:45% [v/v/v]) for 15 min. Invasive cells were scored by counting 10 × 20 magnification fields per filter with a Zeiss Imager Z1 microscope using a 20× objective. Mouse embryonic fibroblast NIH/3T3 cells were routinely included as a positive control. Results are expressed as mean ± SD from three independent experiments.

Western blotting

Cells were lysed with a buffer containing 1% Triton X-100, 1% NP-40, and protease and phosphatase inhibitor cocktails

(Calbiochem/EMD Millipore) in PBS, and the lysates were clarified by centrifugation at 16,000*g* for 15 min. Protein concentration was determined using the BCA Protein Assay kit (Thermo Scientific) according to the manufacturer's instructions. Protein samples were mixed with electrophoresis sample buffer containing 5% (v/v) 2-β-mercaptoethanol and 5% (v/v) bromophenol blue and boiled for 5 min at 95°C. Samples were loaded in equal amounts into precast 4%–20% gradient polyacrylamide gels (Invitrogen) and separated by SDS-PAGE. Resolved proteins were transferred to a nitrocellulose membrane (Whatman) at 130 V for 90 min, followed by blocking of nonspecific binding with 5% BSA in 0.05% Tween-20/PBS for 1 h at room temperature. The membranes were probed with primary antibodies specific to each protein overnight at 4°C and then with HRP-conjugated secondary antibodies (Thermo Scientific and Santa Cruz Biotechnology). Blots were visualized with an ECL detection system (Thermo Scientific) according to the manufacturer's instructions, and chemiluminescent signal was captured with a FluorChem IS-8900 (Alpha Innotech). Each Western blot was done at least three times, and here we show representative experiments.

Co-IP

For co-IP of Flag-tagged MMP3 protein complexes, CM was incubated with anti-Flag M2 antibody-conjugated agarose beads (F2426, Sigma) for 16 h at 4°C. The beads were then washed three times with 0.05% Tween/PBS, and the immune complexes were directly eluted with electrophoresis sample buffer and analyzed by Western blotting. For liquid chromatography-tandem mass spectrometry (LC-MS/MS) analysis, beads were washed with 0.05% Tween/PBS, and protein complexes were eluted with a Flag peptide (F3290, Sigma) in 0.05% Tween/PBS. Samples were then precipitated with trichloroacetic acid and reconstituted with a buffer (Invitrosol, MS10007, Invitrogen) suitable for mass spectrometry analysis.

For co-IP of HSP90β protein complexes, CM was incubated with 10 μg of control rabbit IgG or anti-HSP90β antibody for 16 h at 4°C. Precipitation was performed with protein G sepharose beads (17-0618-01, GE Healthcare) for 4 h at 4°C. The beads were then washed three times with 0.05% Tween/PBS, and the immune complexes were directly eluted with electrophoresis sample buffer and analyzed by Western blotting.

Mass spectrometry analysis

Mass spectrometry analysis is described in the Supplemental Material. Scaled signal intensities were log2 transformed and analyzed by R software.

Statistical analysis

Statistical analyses were performed using GraphPad Prism 5.0 software. Student's *t*-test (unpaired with Welch's correction, two-tailed, 95% confidence interval) was used to determine statistical significance. Statistical analyses were always performed in relation to vector control cells (unless stated otherwise).

Acknowledgments

References

Carpenter AE, Jones TR, Lamprecht MR, Clarke C, Kang IH, Friman O, Guertin DA, Chang JH, Lindquist RA, Moffat J, et al. 2006. CellProfiler: Image analysis software for identifying and quantifying cell phenotypes. *Genome Biol* **7:** R100.

Catelli MG, Ramachandran C, Gauthier Y, Legagneux V, Quelard C, Baulieu EE, Shyamala G. 1989. Developmental regulation of murine mammary-gland 90 kDa heat-shock proteins. *Biochem J* **258:** 895–901.

Cheng CF, Fan J, Fedesco M, Guan S, Li Y, Bandyopadhyay B, Bright AM, Yerushalmi D, Liang M, Chen M, et al. 2008. Transforming growth factor α (TGFα)-stimulated secretion of HSP90α: Using the receptor LRP-1/CD91 to promote human skin cell migration against a TGFβ-rich environment during wound healing. *Mol Cell Biol* **28:** 3344–3358.

Cowen LE, Lindquist S. 2005. Hsp90 potentiates the rapid evolution of new traits: Drug resistance in diverse fungi. *Science* **309:** 2185–2189.

de Graauw M, Tijdens I, Smeets MB, Hensbergen PJ, Deelder AM, van de Water B. 2008. Annexin A2 phosphorylation mediates cell scattering and branching morphogenesis via cofilin Activation. *Mol Cell Biol* **28:** 1029–1040.

Desprez P, Roskelley C, Campisi J, Bissell MJ. 1993. Isolation of functional cell lines from a mouse mammary epithelial cell strain: The importance of basement membrane and cell-cell interaction. *Mol Cell Differ* **1:** 99–110.

Dufour A, Sampson NS, Zucker S, Cao J. 2008. Role of the hemopexin domain of matrix metalloproteinases in cell migration. *J Cell Physiol* **217:** 643–651.

Eustace BK, Sakurai T, Stewart JK, Yimlamai D, Unger C, Zehetmeier C, Lain B, Torella C, Henning SW, Beste G, et al. 2004. Functional proteomic screens reveal an essential extracellular role for hsp90α in cancer cell invasiveness. *Nat Cell Biol* **6:** 507–514.

Farina AR, Tacconelli A, Cappabianca L, Gulino A, Mackay AR. 2002. Inhibition of human MDA-MB-231 breast cancer cell invasion by matrix metalloproteinase 3 involves degradation of plasminogen. *Eur J Biochem* **269:** 4476–4483.

Fata JE, Werb Z, Bissell MJ. 2004. Regulation of mammary gland branching morphogenesis by the extracellular matrix and its remodeling enzymes. *Breast Cancer Res* **6:** 1–11.

Fata JE, Mori H, Ewald AJ, Zhang H, Yao E, Werb Z, Bissell MJ. 2007. The MAPK(ERK-1,2) pathway integrates distinct and antagonistic signals from TGFα and FGF7 in morphogenesis of mouse mammary epithelium. *Dev Biol* **306:** 193–207.

Fotouhi N, Lugo A, Visnick M, Lusch L, Walsky R, Coffey JW, Hanglow AC. 1994. Potent peptide inhibitors of stromelysin based on the prodomain region of matrix metalloproteinases. *J Biol Chem* **269:** 30227–30231.

Glasheen BM, Kabra AT, Page-McCaw A. 2009. Distinct functions for the catalytic and hemopexin domains of a *Drosoph-*

ila matrix metalloproteinase. *Proc Natl Acad Sci* **106:** 2659–2664.

Hirai Y, Lochter A, Galosy S, Koshida S, Niwa S, Bissell MJ. 1998. Epimorphin functions as a key morphoregulator for mammary epithelial cells. *J Cell Biol* **140:** 159–169.

Houghton AM, Hartzell WO, Robbins CS, Gomis-Ruth FX, Shapiro SD. 2009. Macrophage elastase kills bacteria within murine macrophages. *Nature* **460:** 637–641.

Iioka H, Ueno N, Kinoshita N. 2004. Essential role of MARCKS in cortical actin dynamics during gastrulation movements. *J Cell Biol* **164:** 169–174.

Khokha R, Werb Z. 2011. Mammary gland reprogramming: Metalloproteinases couple form with function. *Cold Spring Harb Perspect Biol* **3:** a0044333.

Kouros-Mehr H, Werb Z. 2006. Candidate regulators of mammary branching morphogenesis identified by genome-wide transcript analysis. *Dev Dyn* **235:** 3404–3412.

Li W, Li Y, Guan S, Fan J, Cheng CF, Bright AM, Chinn C, Chen M, Woodley DT. 2007. Extracellular heat shock protein-90α: Linking hypoxia to skin cell motility and wound healing. *EMBO J* **26:** 1221–1233.

Lochter A, Galosy S, Muschler J, Freedman N, Werb Z, Bissell MJ. 1997a. Matrix metalloproteinase stromelysin-1 triggers a cascade of molecular alterations that leads to stable epithelial-to-mesenchymal conversion and a premalignant phenotype in mammary epithelial cells. *J Cell Biol* **139:** 1861–1872.

Lochter A, Srebrow A, Sympson CJ, Terracio N, Werb Z, Bissell MJ. 1997b. Misregulation of stromelysin-1 expression in mouse mammary tumor cells accompanies acquisition of stromelysin-1-dependent invasive properties. *J Biol Chem* **272:** 5007–5015.

Lu P, Werb Z. 2008. Patterning mechanisms of branched organs. *Science* **322:** 1506–1509.

Maroun CR, Naujokas MA, Holgado-Madruga M, Wong AJ, Park M. 2000. The tyrosine phosphatase SHP-2 is required for sustained activation of extracellular signal-regulated kinase and epithelial morphogenesis downstream from the met receptor tyrosine kinase. *Mol Cell Biol* **20:** 8513–8525.

Mori H, Tomari T, Koshikawa N, Kajita M, Itoh Y, Sato H, Tojo H, Yana I, Seiki M. 2002. CD44 directs membrane-type 1 matrix metalloproteinase to lamellipodia by associating with its hemopexin-like domain. *EMBO J* **21:** 3949–3959.

Mori H, Lo AT, Inman JL, Alcaraz J, Ghajar CM, Mott JD, Nelson CM, Chen CS, Zhang H, Bascom JL, et al. 2013. Transmembrane/cytoplasmic, rather than catalytic, domains of Mmp14 signal to MAPK activation and mammary branching morphogenesis via binding to integrin β1. *Development* **140:** 343–352.

Noe V, Fingleton B, Jacobs K, Crawford HC, Vermeulen S, Steelant W, Bruyneel E, Matrisian LM, Mareel M. 2001. Release of an invasion promoter E-cadherin fragment by matrilysin and stromelysin-1. *J Cell Sci* **114:** 111–118.

Overall CM, Kleifeld O. 2006. Tumour microenvironment—opinion: Validating matrix metalloproteinases as drug targets and anti-targets for cancer therapy. *Nat Rev Cancer* **6:** 227–239.

Queitsch C, Sangster TA, Lindquist S. 2002. Hsp90 as a capacitor of phenotypic variation. *Nature* **417:** 618–624.

Radisky DC, Levy DD, Littlepage LE, Liu H, Nelson CM, Fata JE, Leake D, Godden EL, Albertson DG, Nieto MA, et al. 2005. Rac1b and reactive oxygen species mediate MMP-3-induced EMT and genomic instability. *Nature* **436:** 123–127.

Reichmann E, Ball R, Groner B, Friis RR. 1989. New mammary epithelial and fibroblastic cell clones in coculture form structures competent to differentiate functionally. *J Cell Biol* **108:** 1127–1138.

Rutherford SL, Lindquist S. 1998. Hsp90 as a capacitor for morphological evolution. *Nature* **396:** 336–342.

Sakamoto T, Seiki M. 2009. Cytoplasmic tail of MT1-MMP regulates macrophage motility independently from its protease activity. *Genes Cells* **14:** 617–626.

Schnelzer A, Prechtel D, Knaus U, Dehne K, Gerhard M, Graeff H, Harbeck N, Schmitt M, Lengyel E. 2000. Rac1 in human breast cancer: Overexpression, mutation analysis, and characterization of a new isoform, Rac1b. *Oncogene* **19:** 3013–3020.

Sharp SY, Boxall K, Rowlands M, Prodromou C, Roe SM, Maloney A, Powers M, Clarke PA, Box G, Sanderson S, et al. 2007. In vitro biological characterization of a novel, synthetic diaryl pyrazole resorcinol class of heat shock protein 90 inhibitors. *Cancer Res* **67:** 2206–2216.

Simian M, Hirai Y, Navre M, Werb Z, Lochter A, Bissell MJ. 2001. The interplay of matrix metalloproteinases, morphogens and growth factors is necessary for branching of mammary epithelial cells. *Development* **128:** 3117–3131.

Sims JD, McCready J, Jay DG. 2011. Extracellular heat shock protein (Hsp)70 and Hsp90α assist in matrix metalloproteinase-2 activation and breast cancer cell migration and invasion. *PLoS ONE* **6:** e18848.

Sternlicht MD, Lochter A, Sympson CJ, Huey B, Rougier JP, Gray JW, Pinkel D, Bissell MJ, Werb Z. 1999. The stromal proteinase MMP3/stromelysin-1 promotes mammary carcinogenesis. *Cell* **98:** 137–146.

Sympson CJ, Talhouk RS, Alexander CM, Chin JR, Clift SM, Bissell MJ, Werb Z. 1994. Targeted expression of stromelysin-1 in mammary gland provides evidence for a role of proteinases in branching morphogenesis and the requirement for an intact basement membrane for tissue-specific gene expression. *J Cell Biol* **125:** 681–693.

Taipale M, Jarosz DF, Lindquist S. 2010. HSP90 at the hub of protein homeostasis: Emerging mechanistic insights. *Nat Rev Mol Cell Biol* **11:** 515–528.

Talhouk RS, Chin JR, Unemori EN, Werb Z, Bissell MJ. 1991. Proteinases of the mammary gland: Developmental regulation in vivo and vectorial secretion in culture. *Development* **112:** 439–449.

Talhouk RS, Bissell MJ, Werb Z. 1992. Coordinated expression of extracellular matrix-degrading proteinases and their inhibitors regulates mammary epithelial function during involution. *J Cell Biol* **118:** 1271–1282.

Tam EM, Wu YI, Butler GS, Stack MS, Overall CM. 2002. Collagen binding properties of the membrane type-1 matrix metalloproteinase (MT1-MMP) hemopexin C domain. The ectodomain of the 44-kDa autocatalytic product of MT1-MMP inhibits cell invasion by disrupting native type I collagen cleavage. *J Biol Chem* **277:** 39005–39014.

Thomasset N, Lochter A, Sympson CJ, Lund LR, Williams DR, Behrendtsen O, Werb Z, Bissell MJ. 1998. Expression of autoactivated stromelysin-1 in mammary glands of transgenic mice leads to a reactive stroma during early development. *Am J Pathol* **153:** 457–467.

Vincent-Salomon A, Thiery JP. 2003. Host microenvironment in breast cancer development: Epithelial–mesenchymal transition in breast cancer development. *Breast Cancer Res* **5:** 101–106.

Voss AK, Thomas T, Gruss P. 2000. Mice lacking HSP90β fail to develop a placental labyrinth. *Development* **127:** 1–11.

Wang P, Nie J, Pei D. 2004. The hemopexin domain of membrane-type matrix metalloproteinase-1 (MT1-MMP) is not required for its activation of proMMP2 on cell surface but is essential for MT1-MMP-mediated invasion in three-dimensional type I collagen. *J Biol Chem* **279:** 51148–51155.

Williams JM, Daniel CW. 1983. Mammary ductal elongation: Differentiation of myoepithelium and basal lamina during branching morphogenesis. *Dev Biol* **97:** 274–290.

Wiseman BS, Sternlicht MD, Lund LR, Alexander CM, Mott J, Bissell MJ, Soloway P, Itohara S, Werb Z. 2003. Site-specific inductive and inhibitory activities of MMP-2 and MMP-3 orchestrate mammary gland branching morphogenesis. *J Cell Biol* **162:** 1123–1133.

Witty JP, Wright JH, Matrisian LM. 1995. Matrix metalloproteinases are expressed during ductal and alveolar mammary morphogenesis, and misregulation of stromelysin-1 in transgenic mice induces unscheduled alveolar development. *Mol Biol Cell* **6:** 1287–1303.